THERMAL CONDUCTIVITY OF THE MARTIAN REGOLITH AT THE INSIGHT LANDING SITE FROM HP³ ACTIVE HEATING EXPERIMENTS. M. Grott[1], T. Spohn[1,2], J. Knollenberg[1], C. Krause[3], S. Nagihara[4], P. Morgan[5], S. Piqueux[6], N. Müller[1], M. Golombek[6], J. Murphy[7], M. Siegler[8,9], S. King[7], T.L. Hudson[6], C. Vrettos[10], S.E. Smrekar[6], W.B. Banerdt[6], [1]German Aerospace Center (DLR), Berlin, Germany (Matthias.Grott@dlr.de), [2]International Space Science Institute (ISSI), Bern, Switzerland, [3]German Aerospace Center (DLR), Cologne, Germany, [4]Department of Geosciences, Texas Tech University, Lubbock, USA, [5]Colorado Geological Survey, Colorado School of Mines, Golden, USA, [6]Jet Propulsion Laboratory, California Institute of Technology, Pasadena, USA, [7]Virginia Polytechnic Institute and State University, Blacksburg, USA, [8]Planetary Science Institute, Tucson, AZ, USA, [9]Southern Methodist University, Dallas, TX, USA, [10]Technical University Kaiserslautern, Germany.

Introduction: The InSight Mars mission landed in Homestead hollow in the Elysium Planitia region of Mars at 4.50°N, 135.62°E on Nov. 3rd, 2018 [1]. The Heat Flow and Physical Properties Package (HP³) is part of the InSight payload and is designed to emplace sensors into the martian regolith to measure regolith thermal conductivity and the geothermal gradient in the 0-5 m depth range [2]. Due to unexpected soil properties, the lander's robotic arm needed to assist in probe emplacement. We estimate the mole's back-cap to be 2-3 cm below the surface during the measurement, and since the mole is 40 cm long and inclined 30° with respect to vertical, the mole tip is likely at 37 cm depth.

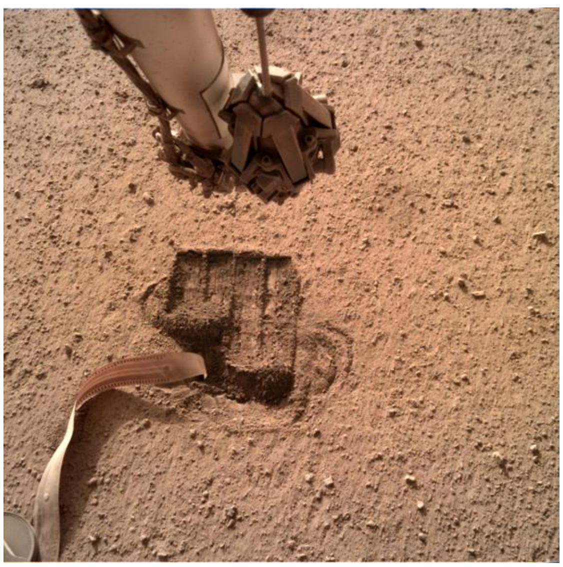

Fig. 1: The HP³ mole after successful burial. The image was taken on Sol 674 and shows the configuration during the active heating experiment.

Measurement: HP³ measures thermal conductivity using its mole as a modified line heat source [3]. In this approach, the probe is heated using known power while simultaneously measuring the resulting temperature rise. Using laboratory-verified numerical models of the mole's response to heating, regolith properties can then be determined.

Here we report on the results of a thermal conductivity measurement conducted between sols 680 and 682. The measurement configuration is shown in Fig. 1. The mole is fully buried, minimizing the influence of diurnal peak-to-peak temperature fluctuations and providing good thermal coupling to the surrounding regolith. The diurnal temperature amplitude measured on sols 680 and 681 at the mole was 3 K and was subtracted from the data of the active heating experiment, which was conducted between 21:00 LTST on sol 681 and 21:00 LTST on sol 682.

Data Analysis: Due to the finite length of the mole, classical methods for data inversion [4] cannot be applied, and we use a finite element model of the mole and regolith to determine thermal conductivity from the measured heating curve [3]. In the model, regolith thermal conductivity, regolith density, and thermal contact conductance between mole and regolith are treated as free parameters, and the root mean square (rms) difference between modeled and measured temperature rise is evaluated between 100 and 1300 min to minimize the influence of transient effects during initial heating.

A Monte-Carlo simulation varying these parameters between 0.02-0.06 W m^{-1} K^{-1}, 600-1800 kg m^{-3}, and 3-250 W m^{-2} K^{-1} was then performed, and all models showing a rms misfit below 0.17 K were accepted. The measured heating curve corrected for background temperature fluctuations is shown in the top panel of Fig. 2 together with the estimated measurement uncertainty and the best fitting numerical model determined from the Monte-Carlo simulations. The best fitting thermal conductivity is 0.039 W m^{-1} K^{-1}, and the rms misfit of this model is 0.07 K.

Results: A histogram of the admissible thermal conductivities is shown in the bottom panel of Fig. 2, and thermal conductivity was found to be 0.039±0.001 W m^{-1} K^{-1}. Taking calibration uncertainties [3] into account, total uncertainty is 0.002 W m^{-1} K^{-1}. Regolith densities compatible with the data span the range between 800 and 1800 kg m^{-3} with a median density of 1095 kg m^{-3} and a 25th and 75th percentile of 997 and 1258 kg m^{-3} respectively.

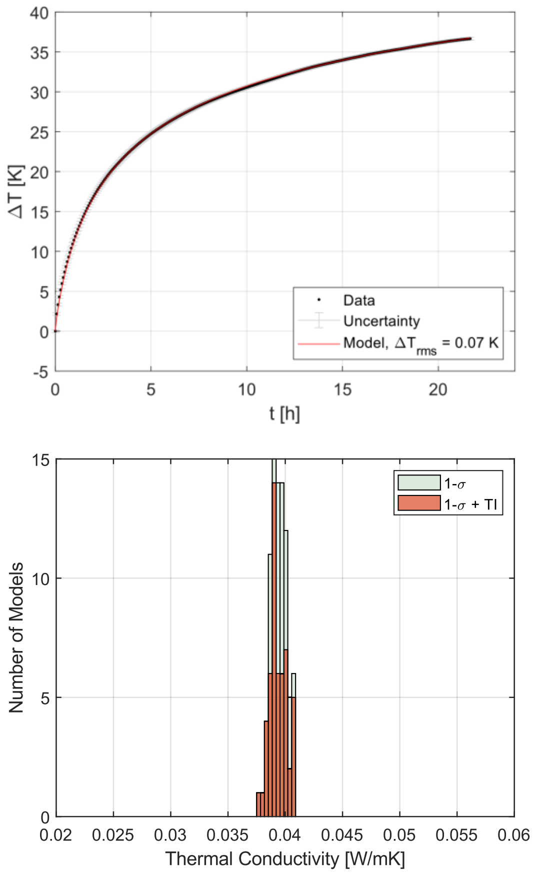

Fig. 2: Top: Temperature rise during the heating experiment as a function of time together with the best fitting model. Measurement uncertainty is indicated in shades. Bottom: Results of the Monte-Carlo simulations showing the permissible thermal conductivities fitting the heating curve constraint (green) as well as a subset of those models also fitting the thermal inertia constraint (red). For comparison, thermal conductivity at the Phoenix landing site was measured to be 0.085 W m^{-1} K^{-1} [5].

An additional constraint that can be applied to these results is the thermal inertia at the landing site, which was determined using the InSight radiometer [1]. Assuming that regolith properties in the depth range probed by the radiometer do not significantly deviate from those in the 0.03 to 0.38 m depth range, regolith density can be further constrained. Requiring the thermal inertia derived from the conductivities and densities above to be between 160 and 230 J m^{-2} K^{-1} s$^{-1/2}$, the median density is found to be 1210 kg m^{-3} with 25th and 75th percentiles of 1108 and 1429 kg m^{-3}, respectively. Densities below 1000 kg m^{-3} can be ruled out. As is evident from Fig. 2, thermal conductivities remain largely unaffected by this additional constraint.

Discussion: Thermal conductivity is often interpreted in terms of regolith grain size by comparing results with laboratory experiments under martian atmospheric conditions [6]. For polydisperse mixtures as encountered in natural soils, the derived grain sizes correspond to the larger grains in the mixture, with 85% to 95% of all particles being smaller than the size determined [7]. For a thermal conductivity of 0.039±0.002 W m^{-1} K^{-1}, grain sizes determined using the scaling laws of [6] are 125-160 µm, corresponding to sand-sized particles. However, this estimate is only valid if cementation is assumed to be minimal. This seems to contradict the fact that clods of soil are present and that steep walls have been found under the InSight lander and surrounding the mole cavity.

Depending on its spatial distribution, cement can have a large influence on thermal conductivity by increasing grain-to-grain contact areas. If deposited on necks between grains, already 0.02% of cement by volume can increase the regolith bulk conductivity by a factor of 2 [8], which would suggest grain sizes of 25-40 µm (dust-sized particles). However, such small particle sizes are implausible, as Homestead hollow appears to be filled by eolian deposits and the maximum saltation limit for particles that can be mobilized by winds is in the 100-600 µm diameter range [9]. Therefore, it seems more likely that cement present in the regolith acts to increase cohesion but has little influence on grain-to-grain contact areas, potentially by being distributed in the form of thin veneers coating the grains rather than cementing necks [8]. Thus, the particle size estimates above would remain largely unchanged.

The regolith densities estimated here are comparable to those derived for other landing sites [10]. Assuming typical bulk densities representative for basaltic martian meteorites of 3250 kg m^{-3}, median densities of 1200 kg m^{-3} derived here would correspond to a bulk porosity of 60%. While this may appear very large, it is consistent with the facts that mole hammering action during the early phases of probe insertion created a significant hole by compacting void spaces [1].

References: [1] Golombek et al., *Nature Comm.*, 11, 1014, 2020. [2] Spohn et al., *SSR*, 214(5), 96, 2018. [3] Grott et al., *ESS*, 6(12), 2556-2574, 2020. [4] Jaeger, *Austr. J. Phys.*, 9, 167, 1956. [5] Zent et al., *JGR*, 115(2), E00E14, 2010. [6] Presley and Christensen, *JGR*, 102(E4), 9221-9230, 1997. [7] Presley and Craddock, *JGR*, 111(E9), E09013, 2006. [8] Piqueux and Christensen, *JGR*, 114(E9), E09006, 2009. [9] Kok et al., *Rep. Prog. Phys.*, 75(10), 106901, 2012. [10] Golombek et al., *The martian surface - composition, mineralogy, and physical properties*, p. 468, 2008.